



Article

Activation of Voltage-Gated Na⁺ Current by GV-58, a Known Activator of Ca_v Channels

Hsin-Yen Cho ¹, Pei-Chun Chen ^{1,2} , Tzu-Hsien Chuang ¹, Meng-Cheng Yu ¹ and Sheng-Nan Wu ^{1,2,*}

¹ Department of Physiology, National Cheng Kung University Medical College, Tainan City 70101, Taiwan; s36094083@gs.ncku.edu.tw (H.-Y.C.); pcchen@mail.ncku.edu.tw (P.-C.C.); s36091051@gs.ncku.edu.tw (T.-H.C.); s36101042@gs.ncku.edu.tw (M.-C.Y.)

² Institute of Basic Medical Sciences, National Cheng Kung University Medical College, Tainan City 70101, Taiwan

* Correspondence: snwu@mail.ncku.edu.tw; Tel.: +886-6-2353535-5334; Fax: +886-6-2362780

Abstract: GV-58 ((2R)-2-[(6-[(5-methylthiophen-2-yl)methyl]amino)-9-propyl-9H-purin-2-yl]amino]butan-1-ol) is recognized to be an activator of N- and P/Q-type Ca²⁺ currents. However, its modulatory actions on other types of ionic currents in electrically excitable cells remain largely unanswered. This study was undertaken to explore the possible modifications caused by GV-58 in ionic currents (e.g., voltage-gated Na⁺ current [I_{Na}], A-type K⁺ current [I_{K(A)}], and *erg*-mediated K⁺ current [I_{K(erg)}]) identified from pituitary GH₃ lactotrophs. GH₃ cell exposure to GV-58 enhanced the transient and late components of I_{Na} with varying potencies; consequently, the EC₅₀ values of GV-58 required for its differential increase in peak and late I_{Na} in GH₃ cells were estimated to be 8.9 and 2.6 μM, respectively. The I_{Na} in response to brief depolarizing pulse was respectively stimulated or suppressed by GV-58 or tetrodotoxin, but it failed to be altered by ω-conotoxin MVIID. Cell exposure to this compound increased the recovery of I_{Na} inactivation evoked by two-pulse protocol based on a geometrics progression; however, in its presence, there was a slowing in the inactivation rate of current decay evoked by a train of depolarizing pulses. The existence of GV-58 also resulted in an increase in the amplitude of ramp-induced resurgent and window I_{Na}. The presence of this compound inhibited I_{K(A)} magnitude, accompanied by a shortening in inactivation time course of the current; however, it mildly decreased I_{K(erg)}. Under current-clamp conditions, GV-58 increased the frequency of spontaneous action potentials in GH₃ cells. Moreover, in NSC-34 motor neuron-like cells, the presence of GV-58 not only raised I_{Na} amplitude but also reduced current inactivation. Taken together, the overall work provides a noticeable yet unidentified finding which implies that, in addition to its agonistic effect on Ca²⁺ currents, GV-58 may concertedly modify the amplitude and gating kinetics of I_{Na} in electrically excitable cells, hence modifying functional activities in these cells.

Keywords: GV-58 ((2R)-2-[(6-[(5-methylthiophen-2-yl)methyl]amino)-9-propyl-9H-purin-2-yl]amino]butan-1-ol); voltage-gated Na⁺ current; resurgent Na⁺ current; window Na⁺ current; K⁺ current; current kinetics; pituitary cell; motor neuron-like cell



Citation: Cho, H.-Y.; Chen, P.-C.; Chuang, T.-H.; Yu, M.-C.; Wu, S.-N. Activation of Voltage-Gated Na⁺ Current by GV-58, a Known Activator of Ca_v Channels. *Biomedicines* **2022**, *10*, 721. <https://doi.org/10.3390/biomedicines10030721>

Academic Editors: Celestino Sardu and Shaker A. Mousa

Received: 17 January 2022

Accepted: 17 March 2022

Published: 20 March 2022

Publisher's Note: MDPI stays neutral with regard to jurisdictional claims in published maps and institutional affiliations.



Copyright: © 2022 by the authors. Licensee MDPI, Basel, Switzerland. This article is an open access article distributed under the terms and conditions of the Creative Commons Attribution (CC BY) license (<https://creativecommons.org/licenses/by/4.0/>).

1. Introduction

GV-58 ((2R)-2-[(6-[(5-methylthiophen-2-yl)methyl]amino)-9-propyl-9H-purin-2-yl]amino]butan-1-ol), which was developed as a modification of (R)-roscovitine, has been viewed as an opener of N- and P/Q-type Ca²⁺ channels [1–5]. This compound was presumably thought to slow the closing of the voltage-gated Ca²⁺ (Ca_v) channel, resulting in a large increase in total Ca²⁺ entry during motor nerve action potential activity [1]. Its presence was reported to enhance spontaneous and evoked activity from murine ventral horn cultures on microelectrode arrays [4]. Earlier studies have demonstrated that this

compound is effective for the management of neuromuscular weakness, such as Lambert–Eaton myasthenic syndrome [3,6–9]. However, the issue of whether and how other types of ionic currents could be perturbed by this compound remains largely unknown.

It has been established that nine isoforms (i.e., Na_v1.1–1.9 [or SCN1A–SCN5A and SCN8A–SCN11A]) of voltage-gated Na⁺ (Na_v) channels are expressed in mammalian excitable tissues, which include central or peripheral nervous system and endocrine system [10,11]. The imperative role played by the activity of these channels is to depolarize the membrane and generate the upstroke of the action potential (AP), hence controlling the firing amplitude, frequency, and pattern present in excitable cells [10–12]. Of additional interest, several activators of Na_v channels have been elaborated preferentially to slow the inactivation rate as well as to increase the late component of voltage-gated Na⁺ current (*I*_{Na}), such as tefluthrin, telmisartan, and apocynin [13–15], whereas some Na_v channel inhibitors (e.g., ranolazine and esaxerenone) known to increase the inactivation rate of the current have been demonstrated [16,17]. However, at present, whether the existence of GV-58 is capable of interacting with the Na_v channels to modify the magnitude and gating properties of *I*_{Na} in excitable cells remains not very thoroughly studied, although its effectiveness in stimulating N- and P/Q-type Ca²⁺ currents has been demonstrated [1–5].

In light of the above-mentioned considerations, in this study, the electrophysiological effects of GV-58 and other related compounds in pituitary GH₃ cells were extensively investigated. We sought to (a) evaluate whether the presence of GV-58 causes any modifications in the amplitude and gating of *I*_{Na} intrinsically in GH₃ cells; (b) compare the effect of this compound on the peak and late components of *I*_{Na} activated in response to brief depolarizing pulse; (c) study the effect of GV-58 on *erg*-mediated K⁺ current (*I*_{K(erg)}); (d) assess its possible perturbations on spontaneous APs; and (e) investigate the effect of GV-58 on *I*_{Na} in NSC-34 motor neuron-like cells. Our results provide the evidence to reveal that, notwithstanding its ability to stimulate the activity of voltage-gated Ca²⁺ (Ca_v) channels, the differential stimulation by GV-58 of peak and late *I*_{Na} may participate in its regulation of the electrical behaviors of excitable cells (e.g., GH₃ and NSC-34 cells).

2. Materials and Methods

2.1. Chemicals, Drugs, and Solutions

GV-58 (1402821-41-3, ChEMBL2206242, SChEMBL17628602, (2*R*)-2-[(6-[(5-methylthio phen-2-yl)methyl]amino)-9-propyl-9H-purin-2-yl]amino]butan-1-ol, C₁₈H₂₆N₆OS, <https://pubchem.ncbi.nlm.nih.gov/compound/71463101>, accessed on 1 December 2022), ω-conotoxin MVIID, and tetrodotoxin (TTX) were acquired from Alomone Labs (Genechain, Kaohsiung, Taiwan), while 4-aminopyridine, E-4031, nimodipine, ranolazine, retinoic acid, riluzole, and tetraethylammonium chloride (TEA) were from Sigma-Aldrich (Merck, Taipei, Taiwan). The stock solution of GV-58 was kept under −20 °C for long-term storage. We obtained culture media (e.g., Ham’s F-12 medium), fetal bovine or calf serum, horse serum, L-glutamine, and trypsin/EDTA from Hyclone™ (Thermo Fisher Scientific, Tainan, Taiwan), and all other chemicals, including CsCl, CsOH, CdCl₂, and EGTA, were of laboratory grade and supplied from standard sources.

The external solutions and pipette solutions used in this work are illustrated in Table 1.

Table 1. Composition of normal Tyrode’s solution and the pipette solution used in this study.

Bathing Solution	Purpose or Name	Composition
Bathing solution	Normal Tyrode’s solution	136 mM NaCl, 5.4 mM KCl, 1.8 mM CaCl ₂ , 0.53 mM MgCl ₂ , 5.5 mM glucose, and 5.5 mM HEPES-NaOH buffer, pH 7.4
Bathing solution	High-K ⁺ , Ca ²⁺ -free solution	130 mM KCl, 10 mM NaCl, 3 mM MgCl ₂ , 6 mM glucose, 5 mM HEPES-KOH buffer, pH 7.4

Table 1. Cont.

Bathing Solution	Purpose or Name	Composition
Pipette solution	For recordings of K ⁺ current or membrane potential	130 mM K-aspartate, 20 mM KCl, 1 mM KH ₂ PO ₄ , 1 mM MgCl ₂ , 3 mM Na ₂ ATP, 0.1 mM Na ₂ GTP, 0.1 mM EGTA, and 5 mM HEPES-KOH buffer, pH 7.2
Pipette solution	For recordings of Na ⁺ or Ca ²⁺ current	130 mM Cs-aspartate, 20 mM CsCl, 1 mM KH ₂ PO ₄ , 1 mM MgCl ₂ , 3 mM Na ₂ ATP, 0.1 mM Na ₂ GTP, 0.1 mM EGTA, and 5 mM HEPES-CsOH buffer, pH 7.2

2.2. Cell Preparations

Pituitary GH₃ somatolactotrophs, supplied by the Bioresource Collection and Research Center ([BCRC-60015, <https://catalog.bcrc.firdi.org.tw/BcrcContent?bid=60015>, accessed on 1 December 2022], Hsinchu, Taiwan), were maintained in Ham's F-12 medium, with which 15% heat-inactivated horse serum (*v/v*), 2.5% fetal calf serum (*v/v*), and 2 mM L-glutamine were supplemented. NSC-34 neuronal cells were originally produced by fusion of motor neuron-enriched, embryonic mouse spinal cords with mouse neuroblastoma [12,18]. They underwent growth in a 1:1 mixture of DMEM and Ham's F12 medium with 10% heat-inactivated fetal bovine serum (*v/v*) and 1% penicillin-streptomycin. To slow cell proliferation and enhance their maturation towards a differentiated state, before confluence, we maintained NSC-34 cells in 1:1 DMEM plus Ham's F-12 medium supplemented with 1% fetal bovine serum and 1 μM retinoic acid. GH₃ and NSC-34 cells were grown in monolayer culture in 50 mL plastic culture flasks in a humidified environment of CO₂/air (1:19). Subcultures were made by trypsinization (0.025% trypsin solution [HyClone™] containing 0.01% sodium *N,N*-diethyldithiocarbamate and EDTA). We conducted the electrophysiological measurements when cells reached 60–79% confluence (usually 5–7 days).

2.3. Electrophysiological Measurements

During the few hours before the experiments, we gently dissociated GH₃ or NSC-34 cells with 1% trypsin-EDTA solution and then placed a few drops of cell suspension into a home-made chamber fixed on the working stage of an inverted DM-II fluorescence microscope (Leica; Major Instruments, Tainan, Taiwan). Cells were immersed at room temperature (20–25 °C) in normal Tyrode's solution, the composition of which was detailed in Table 1, and they were allowed to attach to the chamber's bottom. The electrodes that we used to measure were fabricated from Kimax-51 glass tubing with 1.5 mm outer diameter (#34500; Kimble, Dogger, New Taipei City, Taiwan) by using a vertical two-stage puller (PP-830; Narishige, Major Instruments, Tainan, Taiwan). Being filled with different internal solution, the recording electrodes had tip resistances of 3–5 MΩ. During the measurements, the electrode was mounted in an air-tight holder which has a suction port on the side, and a chloride silver was used to be in contact with the internal solution. We recorded ionic currents or membrane potential in the whole-cell configuration of a modified patch-clamp technique with the use of either an Axoclamp-2B (Molecular Devices, Sunnyvale, CA, USA) or an RK-400 amplifier (Bio-Logic, Claix, France), as elaborated elsewhere [13–15]. GΩ-seals were commonly achieved in an all-or-nothing fashion and resulted in a dramatic improvement in signal-to-noise ratio. The liquid junction potentials (−13 ± 1 mV, n = 27), which occur when the ionic compositions in the pipette internal solution and those of bath solution are different, were zeroed shortly before GΩ-seal formation was achieved, and the whole-cell data were then corrected. During measurements, we exchanged the solutions through a home-made gravity-driven type of bath perfusion.

The signals (i.e., current and potential tracings) were monitored at a given interval and digitally stored on-line at 10 kHz in an ASUS ExpertBook laptop computer (P2451F; Yuan-Dai, Tainan, Taiwan). For efficient analog-to-digital (A/D) and digital-to-analog (D/A) conversion to proceed, a Digidata-1440A equipped with a laptop computer was operated by pClamp 10.6 software run under Microsoft Windows 7 (Redmond, WA, USA).

We low-pass filtered current signals at 2 kHz with a FL-4 four-pole Bessel filter (Dagan, Minneapolis, MN, USA). A variety of pClamp-generated voltage-clamp protocols with various rectangular or ramp waveforms were designed and then delivered to the tested cells through D/A conversion in order to determine the current–voltage (I – V) relation of ionic currents specified (Sections 3.3 and 3.10) and the recovery time course of current inactivation (Section 3.4). As pulse-train stimulation was applied to the tested cell, we used an Astro-Med Grass S88X dual output pulse stimulator (Grass, West Warwick, RI, USA).

2.4. Data Analyses

To assess concentration-dependent stimulation of GV-58 on the transient (peak) and late components of I_{Na} , we kept cells bathed in Ca^{2+} -free Tyrode's solution. During the recordings, we voltage-clamped each examined cell at a holding potential of -80 mV, and the brief depolarizing pulse to -10 mV was delivered to evoke peak and late I_{Na} . The late I_{Na} during cell exposure to 100 μ M GV-58 was taken as 100%, and those (i.e., peak and late I_{Na}) acquired in the presence of different GV-58 concentrations (0.3 – 30 μ M) were then compared. The concentration-dependent stimulation by this compound of peak and late I_{Na} in pituitary GH₃ cells were determined by fitting the modified Hill equation. That is,

$$\text{Percentage increase (\%)} = (E_{max} \times [GV-58]^{n_H}) / (EC_{50}^{n_H} + [GV-58]^{n_H})$$

where $[GV-58]$ is the GV-58 concentration applied, n_H the Hill coefficient, EC_{50} the concentration required for a 50% stimulation of peak or late I_{Na} activated in response to rapid depolarizing command voltage, and E_{max} the maximal stimulation of peak or late I_{Na} produced by the existence of GV-58.

The I – V relationship of peak I_{Na} with or without addition of GV-58 was derived and fitted with a Boltzmann function given by:

$$\frac{I}{I_{max}} = \frac{G}{1 + \exp[-(V - V_h)/k]} \times (V - E_{rev})$$

where V is the voltage in mV, E_{rev} the reversal potential of I_{Na} (fixed at $+45$ mV), G the Na^+ conductance in nS, and I the current in pA, while V_h and k are the gating parameters.

2.5. Curve-Fitting Procedures and Statistical Analyses

Curve-fitting (linear or non-linear [e.g., exponential or sigmoidal curve]) to experimental datasets was conducted with the goodness of fit by using different analytical procedures, such as the Microsoft "Solver" built in Excel 2019 (Microsoft), OriginPro[®] 2021 program (OriginLab; Scientific Formosa, Kaohsiung, Taiwan), and MathCad Prime 7 (Otsuka, New Taipei City, Taiwan). The electrophysiological data are presented as the mean \pm standard error of the mean (SEM), with the sample sizes (n) indicating the cell numbers from which the results were acquired. We performed Student's t -tests (for paired or unpaired samples) and analysis of variance (one-way ANOVA or two-way-ANOVA) with or without repeated measures followed by post hoc Fisher's least significance difference test. The statistical calculations were performed by using SPSS 17.0 (AsiaAnalytics, Taipei, Taiwan). A p -value of less than 0.05 was considered to indicate statistical difference.

3. Results

3.1. Stimulatory Effect of GV-58 on Voltage-Gated Na^+ Current Measured from Pituitary GH₃ Cells

For the first stage of measurements, we kept cells bathed in Ca^{2+} -free Tyrode's solution which contained 10 mM tetraethylammonium chloride (TEA) and 0.5 mM $CdCl_2$. TEA and $CdCl_2$ were used to block most of the K^+ and Ca^{2+} currents, respectively. As the depolarizing command voltage from -80 to -10 mV was imposed on the tested cells, we were able to detect an inward current which displayed the rapidly activating and inactivating time course (Figure 1A,B). This type of inward current was, respectively,

sensitive to inhibition or stimulation by tetrodotoxin (1 μM) or tefluthrin (10 μM), and it has hence been identified as a voltage-gated Na^+ current (I_{Na}) [13,17,19]. Of notice, one minute after cells were exposed to GV-58, the amplitude of I_{Na} progressively increased in combination with a slowing in the inactivation time course of the current. For example, the addition of GV-58 markedly increased the peak I_{Na} from 215 ± 21 to 309 ± 29 pA ($n = 8$, $p < 0.05$), and the time constant in the slow component of current inactivation ($\tau_{\text{inact(S)}}$) was concurrently raised to 3.8 ± 0.4 ms from a control of 2.1 ± 0.3 ms ($n = 8$, $p < 0.05$). However, no significant difference in the fast component of current inactivation could be demonstrated. After washout of the compound, current amplitude was returned to 219 ± 23 pA ($n = 7$, $p < 0.05$).

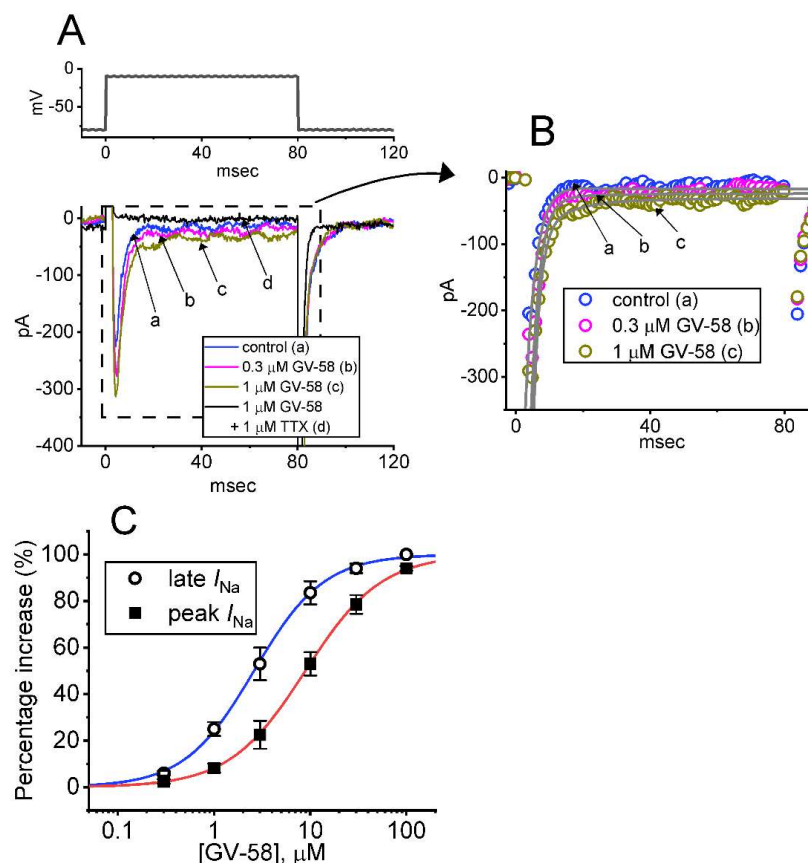


Figure 1. Stimulatory effect of GV-58 on voltage-gated Na^+ current (I_{Na}) in pituitary GH_3 cells. This stage of experiments was conducted in cells which were bathed in Ca^{2+} -free Tyrode's solution, and the solution contained 10 mM tetraethylammonium chloride (TEA) and 0.5 mM CdCl_2 . The recording electrodes that we used were filled up with a Cs^+ -enriched solution. (A) Representative current traces activated by short depolarizing pulse (indicated in the upper part). Current trace labeled "a" was obtained during control (i.e., absence of GV-58), those labeled "b" or "c" were recorded during the exposure to 0.3 or 1 μM GV-58, and that labeled "d" was obtained in the presence of 1 μM GV-58 plus 1 μM tetrodotoxin (TTX). In (B), current traces (indicated in open circles) indicate an expanded record from dashed box of (A) for a higher time resolution. Of note, current trace labeled "d" was skipped. The gray lines overlaid on each trace indicate best fit to the data points with a two-exponential function. (C) Concentration-dependent response of GV-58-mediated stimulation of peak or late I_{Na} residing in GH_3 cells (mean \pm SEM; $n = 8$). The peak and late components of I_{Na} activated in response to the depolarizing pulse from -80 to -10 mV were taken at the start and the end-pulse of the depolarizing command voltage with a duration of 80 ms. The continuous line (blue and red colors) indicates the best fit to a modified Hill equation, as revealed in Materials and Methods.

The relationship between the GV-58 concentration and the peak or late component of I_{Na} evoked in response to abrupt membrane depolarizing was further analyzed and constructed. In this stage of experiments, each cell was rapidly depolarized from -80 to -10 mV, and peak or late I_{Na} measured at varying concentrations (0.3 – 100 μM) of GV-58 were compared. As can be seen in Figure 1C, GH₃ cell exposure to GV-58 resulted in a concentration-dependent rise in the amplitude of peak and late I_{Na} . The EC₅₀ value for GV-58-stimulated peak or late I_{Na} was computed to be 8.9 or 2.6 μM , respectively, and GV-58 at a concentration of 100 μM almost fully increased I_{Na} . The present results, therefore, reflect that GV-58 is capable of exercising a stimulatory action on depolarization-activated I_{Na} in GH₃ cells and that the late component of I_{Na} increases to a greater extent than the peak component of the current in its presence.

3.2. Comparisons of Effects of GV-58, ω -Conotoxin MVIID, and Tetrodotoxin (TTX) on Peak I_{Na}

Earlier studies have been demonstrated to report the effectiveness of GV-58 in enhancing the amplitude of voltage-gated Ca^{2+} currents (e.g., N- and P/Q-type Ca^{2+} currents) [2–5]. We, therefore, explored and compared effects of GV-58, ω -conotoxin MVIID, or TTX on I_{Na} inherently in these cells. ω -Conotoxin MVIID, a small, disulfide-rich peptide purified from the venoms of predatory cone snails, was previously reported to be an inhibitor of N- and P/Q-type Ca^{2+} currents in adrenal chromaffin cells [20]. As summarized in Figure 2, the peak amplitude of I_{Na} was increased in the presence of GV-58; however, it was effectively depressed by cell exposure to TTX (1 μM) but not by ω -conotoxin MVIID (100 nM). Moreover, the amplitude of L-type Ca^{2+} currents ($I_{Ca,L}$) evoked from -50 to $+10$ mV was not affected by ω -conotoxin MVIID (100 nM) or by GV-58 (3 μM). In the continued presence of 3 μM GV-58, further addition of nimodipine (1 μM), an inhibitor of $I_{Ca,L}$, effectively decreased the peak amplitude of $I_{Ca,L}$ by about 90%. Therefore, the I_{Na} evoked in response to brief depolarizing pulse is sensitive to stimulation by GV-58 and to inhibition by TTX, but it remains unaltered in the presence of ω -conotoxin MVIID, suggesting that the magnitude of N- and P/Q-type Ca^{2+} currents is unlikely to be linked to GV-58-stimulated I_{Na} found in GH₃ cells.

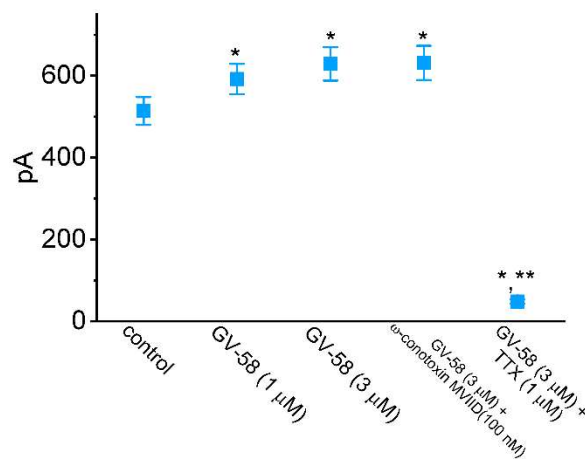


Figure 2. Comparisons of effects of GV-58, GV-58 plus ω -conotoxin MVIID, and GV-58 plus tetrodotoxin (TTX) on the peak amplitude of I_{Na} recorded from GH₃ cells. Cells were immersed in Ca^{2+} -free Tyrode's solution containing 10 mM TEA, and the pipettes used were filled with Cs^{+} -containing solution. Current amplitude was taken at the beginning of the brief depolarizing pulse from -80 to -10 mV. Each bar indicates the mean \pm SEM ($n = 8$ for each bar). Of notice, the peak I_{Na} in GH₃ cells is subject to inhibition by TTX but not by ω -conotoxin MVIID. * Significantly different from control ($p < 0.05$) and ** Significantly different from GV-58 (3 μM) alone group ($p < 0.05$). Statistical analyses were made by one-way ANOVA among different groups ($p < 0.05$).

3.3. Effect of GV-58 on the Steady-State Current–Voltage (I – V) Relationship of Peak I_{Na}

We further examined the steady-state I – V relationships of peak I_{Na} obtained with or without the application of GV-58. These voltage-clamp experiments were conducted in cells held at -80 mV, and a series of voltage pulses between -80 and $+40$ mV was imposed on the tested cells. As shown in Figure 3, the presence of $1 \mu\text{M}$ GV-58 did not alter the overall I – V relationship of peak I_{Na} , although it increased peak amplitude of I_{Na} , particularly at the level of -10 mV. The reversal potential of peak I_{Na} did not differ significantly between the absence and presence of GV-58. The I – V curves obtained in the control period and during exposure to $1 \mu\text{M}$ GV-58 were fitted with a Boltzmann function as stated in Materials and Methods. In control (i.e., the absence of GV-58), $G = 5.5 \pm 0.3$ nS, $V_h = -23.9 \pm 2.1$ mV, $k = 14.9 \pm 1.9$ (n = 8), while in the presence of $1 \mu\text{M}$ GV-58, $G = 7.5 \pm 0.4$ nS, $V_h = -23.6 \pm 1.9$ mV, $k = 14.5 \pm 1.8$ (n = 8). It is, thus, likely that the steady-state activation curve of I_{Na} was not changed during cell exposure to $1 \mu\text{M}$ GV-58.

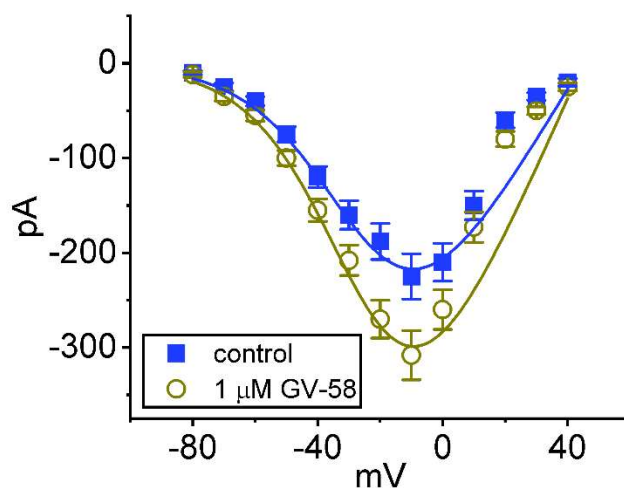


Figure 3. Effect of GV-58 on the steady-state I – V relationship of peak I_{Na} . In these experiments, we voltage-clamped the cells at -80 mV, and various depolarizing pulses from -80 to $+40$ in 10 mV increments were applied to evoke I_{Na} . Current amplitude at each depolarizing pulse was measured at the beginning of the voltage pulse. Data points shown in filled blue squares are control, and those in open brown circles were obtained in the presence of $1 \mu\text{M}$ GV-58. The smooth line taken with or without the GV-58 addition was fitted with a Boltzmann function as detailed in Materials and Methods.

3.4. Effect of GV-58 on the Recovery from I_{Na} Inactivation Evoked during Varying Interpulse Intervals

We next examined whether the existence of GV-58 produces any effect on the recovery of I_{Na} from inactivation by responding to a two-step voltage protocol. In this protocol, a 30 ms step to -10 mV was applied to the examined cell, and another 30 ms conditioning step to -10 mV with varying interpulse intervals inactivated most of the current. The recovery from current inactivation at the holding potential of -80 mV was hence examined at different times with a geometrics progression, as demonstrated in Figure 4A,B. In the control period (i.e., GV-58 was not present), the peak amplitude of I_{Na} nearly completely recovered from inactivation when the interpulse duration reached 1 s. The time constants of recovery from current inactivation acquired in the absence and presence of $10 \mu\text{M}$ GV-58 were least squares fitted by a single-exponential function with the values of 5.34 ± 0.07 and 2.11 ± 0.06 ms (n = 8, $p < 0.05$), respectively. The experimental observations indicate that a conceivable increase in the recovery from inactivation of I_{Na} is seen by adding GV-58.

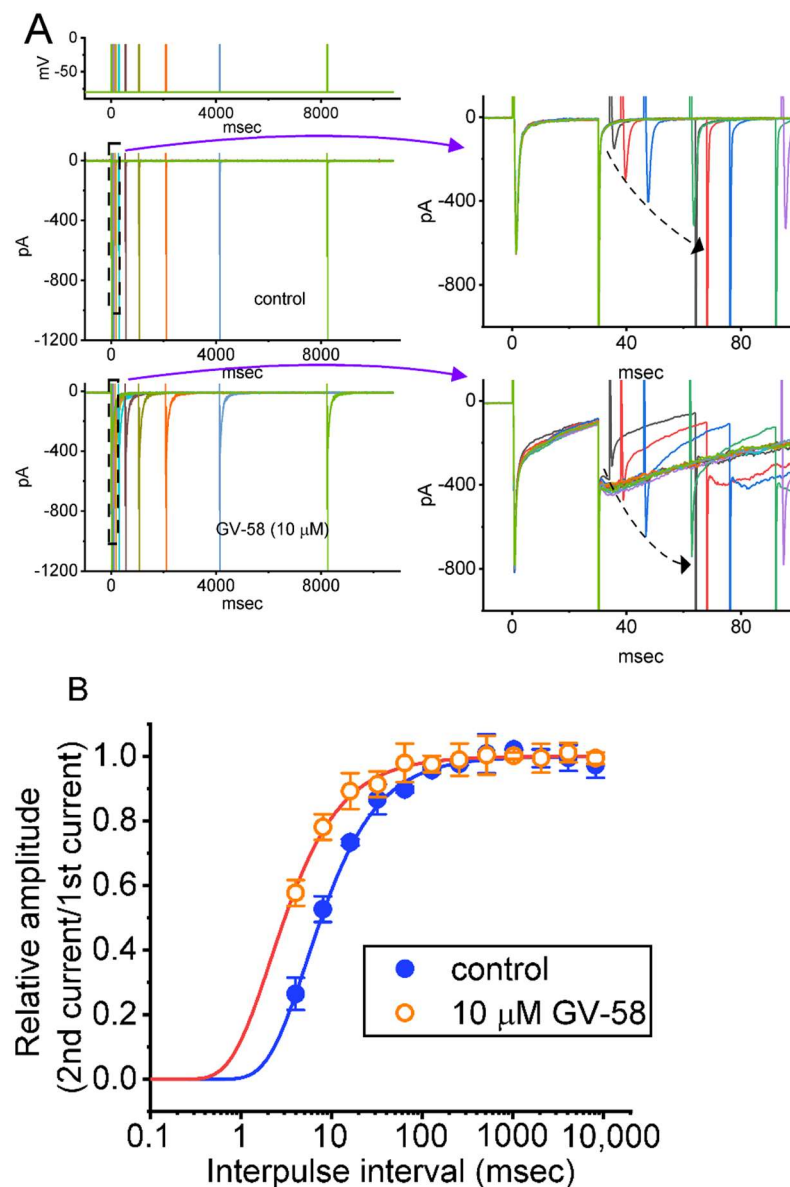


Figure 4. Effect of GV-58 on the recovery of I_{Na} inactivation identified in GH₃ cells. In this set of experiments, as whole-cell configuration was securely established, we applied two-step voltage protocol in a geometrics progression as indicated in the uppermost part of (A). (A) Representative current traces obtained in the absence (upper) and presence of 10 μM GV-58. The panels on the right side, included to show better illustrations, indicate the expanded records from dashed boxes on the left side. The dashed arrow indicates an incremental progression in the trajectory of current inactivation with the increasing interpulse interval. (B) The relationship of interpulse interval versus the relative amplitude taken in the absence (filled blue circles) and presence (open red circles) of 10 μM GV-58 (mean \pm SEM; $n = 8$ for each point). The relative amplitude in the y -axis was obtained by dividing the second amplitude activated by 30 ms depolarizing command voltage from -80 to -10 mV by the first one. Of note, the x -axis is illustrated in a logarithmic scale. The smooth curve in the absence and presence of 10 μM GV-58 was fitted to a single-exponential function with time constants of 5.34 and 2.11 ms, respectively. The presence of GV-58 was noted to result in an evident increase in current recovery (i.e., a reduction of recovery time constant).

3.5. GV-58 Effect on I_{Na} Decay Evoked during a Train of Depolarizing Command Voltages in GH₃ Cells

Previous work has shown the ability of the train of depolarizing pulses to perturb the peak and persistent I_{Na} , which tend to decrease over time in an exponential fashion [21]. We thus made an effort to explore whether GV-58-mediated stimulation of I_{Na} can be perturbed during pulse-train stimulation. In this set of whole-cell current measurements, we delivered a 40 Hz train of depolarizing pulses from -80 to -10 mV to the tested cell. As shown in Figure 5A–C, the slow current inactivation evoked by responding to such pulse-train stimulation was prominently observed. The mean relationship of peak I_{Na} versus the train duration taken with or without the addition of $3 \mu\text{M}$ GV-58 was constructed and then analyzed. It is noticed that the presence of GV-58 results in slowing the time course of current inactivation during such a train of depolarizing pulses. For example, the time constant for I_{Na} during a train of command voltages was measurably increased to 189 ± 23 ms ($n = 7, p < 0.05$) from a control value of 92 ± 12 ms ($n = 7$). It is clear, therefore, that the existence of GV-58 produces a marked increase in the decaying time constant of I_{Na} during a train of depolarizing pulses.

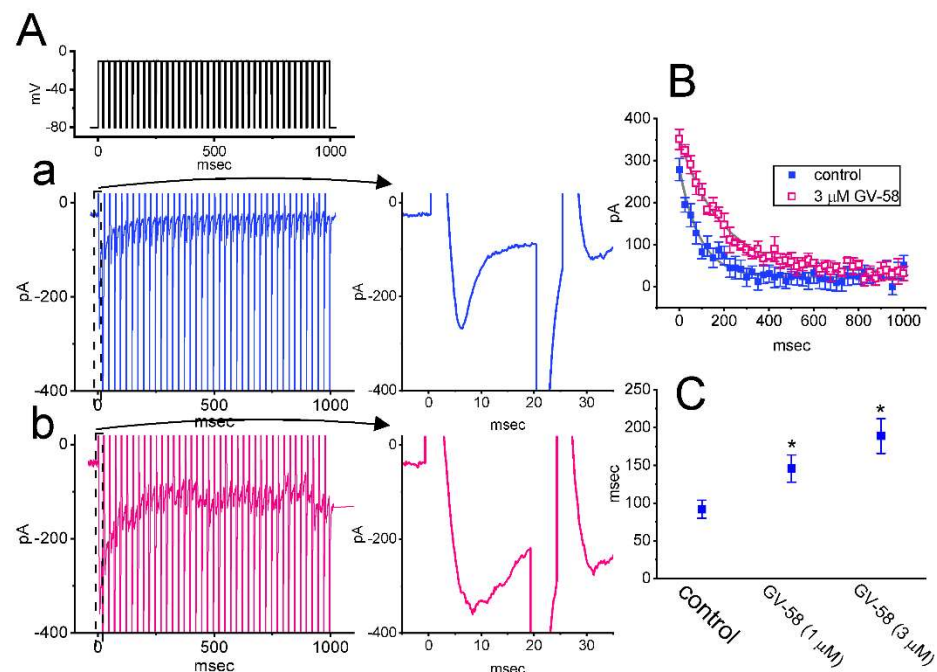


Figure 5. Effect of GV-58 on current decline induced during a 40 Hz train of depolarizing pulses. The train was designed to consist of 40 20 ms pulses separated by 5 ms intervals at -80 mV with a duration of 1 s. (A) Representative current traces obtained in the control period (a) and during cell exposure to $3 \mu\text{M}$ GV-58 (b). The voltage-clamp protocol is illustrated in the uppermost part. To provide single I_{Na} trace, the right side of (A) denotes the expanded records from the dashed box of (Aa) and (Ab). (B) The relationship of peak I_{Na} versus the train duration in the absence (filled blue symbols) and presence (filled red symbols) of $3 \mu\text{M}$ GV-58 (mean \pm SEM; $n = 7$ for each point). The continuous smooth lines over which the data points are overlaid are well fitted by single exponential. Of note, the presence of GV-58 can slow the time course of current inactivation in response to a train of depolarizing pulses. (C) Summary graph showing effect of GV-58 (1 and $3 \mu\text{M}$) on the time constant of current decay in response to a train of depolarizing command voltage from -80 to -10 mV (mean \pm SEM; $n = 7$ for each bar). Current amplitude was measured at the beginning of each depolarizing pulse. Of notice, the presence of GV-58 produces an increase in the time constant in the decline of peak I_{Na} activated by a train of pulses. * Significantly different from control ($p < 0.05$).

3.6. Use-Dependence of GV-58-Induced Stimulation of Peak I_{Na}

This series of whole-cell experiments was conducted to assess the use-dependent property of GV-58-mediated stimulation of peak I_{Na} . As shown in Figure 6, the depolarizing pulses from -80 to -10 mV (30 ms in duration) were applied at 0.2 Hz. Under control conditions (i.e., absence of GV-58), when peak I_{Na} remained active in Ca^{2+} -free Tyrode's solution, the depolarizing pulses were stopped; thereafter, after 25 s of cessation, the depolarizing pulses from -80 to -10 mV at 2 Hz were given to the cells again. The relative amplitude of peak I_{Na} with respect to before the cessation of the depolarizing pulse was constructed and noticed to decline in an exponential fashion. It is illustrated in Figure 5 that peak I_{Na} consisted of both tonic and use-dependent components. For example, in the control period, after a 25 s pause, the peak I_{Na} evoked by the first voltage step or during subsequent repetitive stimuli was suppressed by $11 \pm 3\%$ or $38 \pm 5\%$ ($n = 7$). As cells were exposed to GV-58 ($1 \mu\text{M}$), the peak I_{Na} amplitude at the first depolarizing pulse or during subsequent repetitive pulses were significantly suppressed by $8 \pm 2\%$ or $30 \pm 4\%$, respectively; and the decline in peak I_{Na} became slowed. The results indicated that GV-58-stimulated I_{Na} tends to be composed of two components, namely, tonic and use-dependent components.

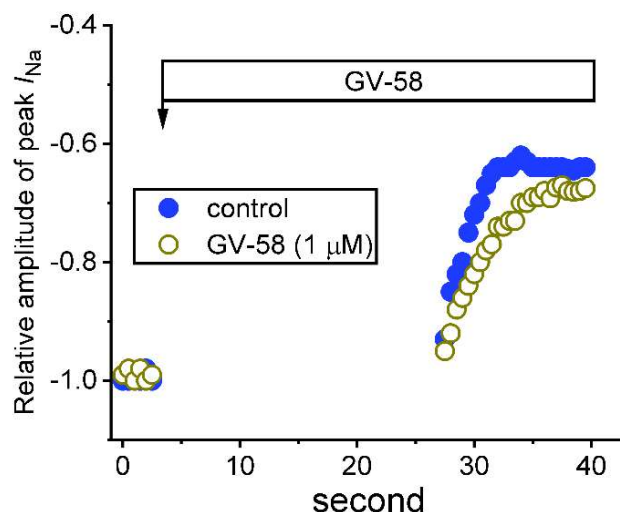


Figure 6. Tonic and use-dependent stimulation of peak I_{Na} by GV-58. The cell was held at -80 mV, and the depolarizing pulse from -80 to -10 mV (30 ms in duration) was applied at 2 Hz. The application of GV-58 ($1 \mu\text{M}$) is illustrated by a horizontal bar shown above. Changes in the relative amplitude of peak I_{Na} with or without the addition of GV-58 ($1 \mu\text{M}$) are illustrated. The peak I_{Na} in the absence (filled circles) or presence (open circles) of GV-58 measured during regular repetitive steps at 0.5 Hz was taken as -1.0 . Immediately after the voltage pulses were stopped, GV-58 ($1 \mu\text{M}$) was added to the bath. The repetitive depolarizing pulses to -10 mV at 2 Hz were applied again 25 s after the cessation of command pulses but still in the continued presence of GV-58 ($1 \mu\text{M}$) (open circles). Of notice, in the presence of GV-58, the peak I_{Na} activated by the first depolarizing step following a pause (around 25 s) had been suppressed to a lesser extent (i.e., tonic stimulation), and, during the repetitive stimuli, the amplitude of peak I_{Na} was further reduced exponentially to a lesser and slower extent (use-dependent stimulation).

3.7. Stimulatory Effect of GV-58 on Resurgent I_{Na} ($I_{Na(R)}$) Seen in GH_3 Cells

The $I_{Na(R)}$ has been recently identified in GH_3 cells [19,22]. Consistent with previous observations in neurons or endocrine cells [22,23], the biophysical property of this current is that it remains undetectable until the membrane potential is repolarized below 0 mV. In addition to being activated by negative voltage steps (i.e., repolarizing steps) rather than positive voltage steps, $I_{Na(R)}$ was noted to activate and decay more slowly than transient I_{Na} . The $I_{Na(R)}$ is thought to help produce rapid depolarization immediately after an

AP and is suited for cells that fire spontaneously at a higher firing rate [23]. For these reasons, we additionally studied whether GV-58 could exert any perturbations on this current. As the whole-cell configuration was securely established, the depolarizing pulse from -80 to $+30$ mV followed by a 300 ms descending (or repolarizing) ramp command voltage to -80 mV was applied to the examined cell. As depicted in Figure 7A,B, the $I_{\text{Na(R)}}$ amplitude activated by this voltage-clamp protocol was evidently increased. For example, the presence of $3 \mu\text{M}$ GV-58 conceivably increased $I_{\text{Na(R)}}$ at -20 mV from 58 ± 3 to 84 ± 7 pA ($n = 7, p < 0.05$). The further addition of ranolazine ($10 \mu\text{M}$), but still in the presence of $3 \mu\text{M}$ GV-58, reduced $I_{\text{Na(R)}}$ amplitude at the same level to 62 ± 5 pA ($n = 7, p < 0.05$). However, the subsequent application of CdCl_2 (0.5 mM) failed to exert any effects on GV-58-stimulated $I_{\text{Na(R)}}$ in GH_3 cells. Ranolazine was previously demonstrated to be an inhibitor of late I_{Na} [16,19].

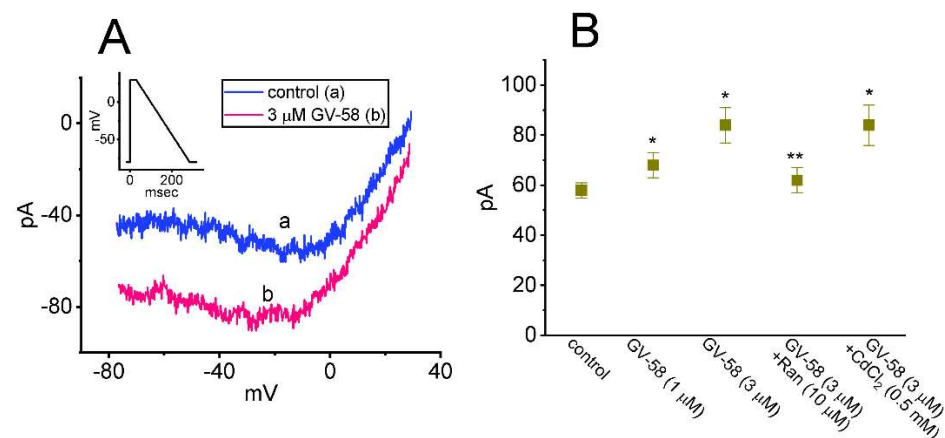


Figure 7. Effect of GV-58 on resurgent I_{Na} ($I_{\text{Na(R)}}$) activated by the downsloping ramp pulse. This set of measurements was conducted in cells bathed in Ca^{2+} -free Tyrode's solution, and we filled up the electrode with Cs^+ -enriched solution. The examined cell was voltage-clamped at -80 mV and the depolarizing pulse to $+30$ mV for 30 ms; thereafter, a slowly descending ramp from $+30$ to -80 mV with a duration of 300 ms (i.e., with a ramp slope of -0.37 mV/ms) was applied to evoke $I_{\text{Na(R)}}$. (A) Representative current traces obtained in the control period (a) and during cell exposure to $3 \mu\text{M}$ GV-58 (b). Inset shows the voltage-clamp protocol delivered. (B) Summary graph showing effect of GV-58, GV-58 plus ranolazine (Ran), and GV-58 plus CdCl_2 on the amplitude of $I_{\text{Na(R)}}$ (mean \pm SEM; $n = 8$ for each bar). Current amplitudes were measured at the level of -20 mV. Of notice, in the continued presence of GV-58, subsequent application of ranolazine, but not of CdCl_2 , effectively suppresses $I_{\text{Na(R)}}$ activated by the descending ramp pulse. * Significantly different from control ($p < 0.05$) and ** significantly different from GV-58 ($3 \mu\text{M}$) alone group ($p < 0.05$). Statistical analyses were performed by one-way ANOVA among different groups ($p < 0.05$).

3.8. Effect of GV-58 on the Window Component of I_{Na} ($I_{\text{Na(W)}}$) Recorded from GH_3 Cells

The presence of instantaneous $I_{\text{Na(W)}}$ has been previously demonstrated in different types of electrically excitable cells [12,24–26]. We continued to explore whether GV-58 presence in GH_3 cells could modify the magnitude of $I_{\text{Na(W)}}$ activated in response to rapid ascending ramp command voltage. In an effort to perform these experiments, we voltage-clamped the tested cell at -80 mV, and we then applied an ascending ramp from -80 to $+20$ mV with a duration of 20 ms to evoke $I_{\text{Na(W)}}$ [26]. As demonstrated in Figure 8A,B, within one minute of exposing cells to GV-58 (1 or $3 \mu\text{M}$), the amplitude of $I_{\text{Na(W)}}$ achieved by the upsloping ramp with a duration of 20 ms was strikingly increased. For example, the existence of $3 \mu\text{M}$ GV-58 evidently increased the peak component of $I_{\text{Na(W)}}$ measured at the level of -20 mV from 378 ± 22 to 498 ± 28 pA ($n = 7, p < 0.05$). After washout of GV-58, current amplitude was returned to 383 ± 24 pA ($n = 7$). However, it needs to be noticed that $I_{\text{Na(W)}}$ measured here was evoked by rapid ramp pulse; it would be unlikely to determine the steady-state activation of I_{Na} . The summary bar graph shown in Figure 8B reveals

that the GV-58 addition is effective in increasing the $I_{Na(W)}$ amplitude and that subsequent addition of 1 μM TTX suppressed GV-58-mediated increase of $I_{Na(W)}$. The present results also imply that GV-58-mediated accentuation of $I_{Na(W)}$ is not mediated through its agonistic effect on Ca_V channels.

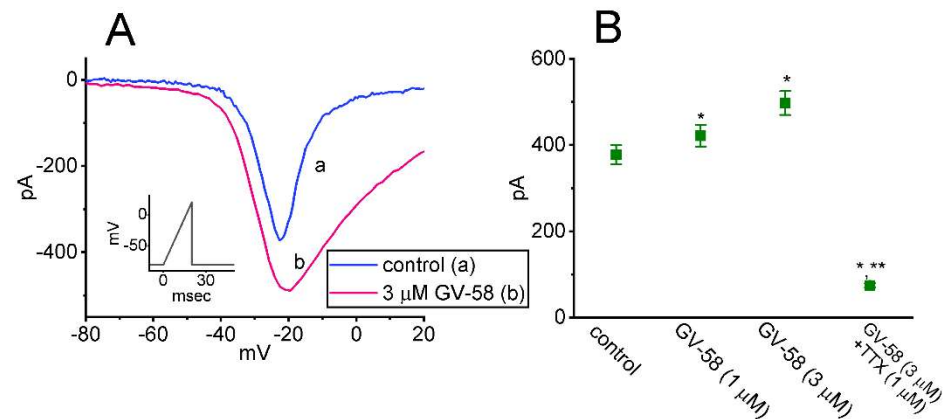


Figure 8. Stimulatory effect of GV-58 on window I_{Na} ($I_{Na(W)}$) activated in response to the upsloping ramp pulse in GH_3 cells. In these experiments, the examined cell was held at -80 mV, and we applied the ascending ramp pulse from -80 - to $+20$ mV with a duration of 20 ms (5 mV/ms) to it. (A) Representative current traces activated by ramp pulse with a duration of 30 ms during the control period (a) and in the presence of 3 μM GV-58 (b). Inset in (A) indicates the voltage-clamp protocol applied. (B) Summary graph showing effect of GV-58 and GV-58 plus tetrodotoxin (TTX) on $I_{Na(W)}$ amplitude identified in GH_3 cells (mean \pm SEM; $n = 8$ for each bar). Current amplitudes measured at the level of -20 mV were taken. * Significantly different from control ($p < 0.05$) and ** Significantly different from GV-58 (3 μM) alone group ($p < 0.05$). Statistical analyses were made by one-way ANOVA ($p < 0.05$). Notably, in the continued presence of GV-58, subsequent addition of TTX effectively suppresses the magnitude of $I_{Na(W)}$ activated in response to brief ascending ramp pulse.

3.9. Inhibitory Effect of GV-58 on A-Type K^+ Current ($I_{K(A)}$) in GH_3 Cells

The suppression of K^+ currents was shown to be effective in improving synaptic impairment or muscle weakness in Lambert–Eaton myasthenic syndrome [3,27]. In another separate set of whole-cell current recordings, different types of ionic currents (e.g., $I_{K(A)}$) were also further examined with respect to possible modifications of GV-58 on them. In these experiments, we bathed cells in Ca^{2+} -free Tyrode's solution containing 1 μM TTX and 0.5 mM CdCl_2 , while the recording electrode was filled up with K^+ -containing solution. The tested cells were voltage-clamped at -80 mV, and the depolarizing command voltage to 0 mV with a duration of 1 s was delivered to evoke a unique type of K^+ outward current with rapid activation and inactivation, which is referred to as A-type K^+ current ($I_{K(A)}$) [28]. One minute after cells were exposed to GV-58 (1 or 3 μM), the amplitude of $I_{K(A)}$ was found to be conceivably decreased; concurrently, the time constant in the slow component of current inactivation ($\tau_{\text{inact}(S)}$) was reduced (Figure 9A–C). For example, the addition of 3 μM GV-58 decreased peak $I_{K(A)}$ amplitude from 423 ± 23 to 121 ± 14 pA ($n = 8$, $p < 0.05$), and it concomitantly reduced the $\tau_{\text{inact}(S)}$ value from 56 ± 7 to 12 ± 3 ms ($n = 8$, $p < 0.05$). The presence of 5 mM 4-aminopyridine fully suppressed the amplitude of $I_{K(A)}$ in GH_3 cells. Results from these observations reflect that, like the action of 4-aminopyridine on $I_{K(A)}$ described previously [28,29], GV-58 per se is capable of decreasing $I_{K(A)}$ and the $\tau_{\text{inact}(S)}$ value of the current found in GH_3 cells.

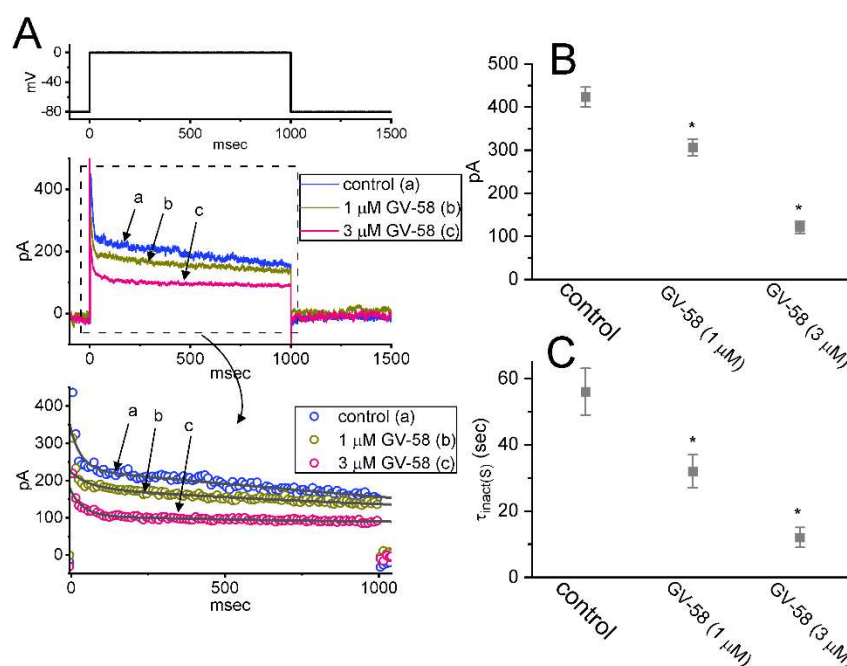


Figure 9. Inhibitory effect of GV-58 on A-type K^+ current ($I_{K(A)}$) in GH₃ cells. Cells were bathed in Ca^{2+} -free Tyrode's solution containing 1 μ M TTX, and we filled up the pipette with K^+ -enriched solution. (A) Represent current traces obtained in the control period ("a", i.e., absence of GV-58) and during cell exposure to 1 μ M GV-58 (b) or 3 μ M GV-58 (c). The uppermost part shows the voltage-clamp protocol applied. The lower part in (A) shows an expanded record from the dashed box, while the data points (circle symbols) were reduced by 50 for better illustration. The smooth line in the lower part represents best fit to two-exponential function (i.e., fast and slow components in current inactivation). Summary graphs appearing in (B,C) demonstrate inhibitory effects of GV-58 (1 or 3 μ M) on peak amplitude and slow component inactivation time constant ($\tau_{inact(S)}$) of $I_{K(A)}$, respectively (mean \pm SEM; $n = 8$ for each bar). * Significantly different from controls ($p < 0.05$). Current amplitude was taken at the start of each depolarizing command voltage from -80 to 0 mV with a duration of 1 s. Of notice, cell exposure to GV-58 is capable of decreasing both peak $I_{K(A)}$ and the $\tau_{inact(S)}$ value of the current in these cells.

3.10. Mild Suppression of Erg-Mediated K^+ Current ($I_{K(erg)}$) Produced by GV-58

In another set of experiments, we further examined the effect of GV-58 on $I_{K(erg)}$ in GH₃ cells. This set of measurements was conducted in cells bathed in high- K^+ , Ca^{2+} -free solution which contained 1 μ M TTX, and the electrode was filled with K^+ -containing solution. The tested cell was maintained in -10 mV, and different command voltages ranging between -90 and 0 mV with a duration of 1 s were applied to evoke hyperpolarization-evoked $I_{K(erg)}$ [30,31]. During cell exposure to 3 μ M GV-58, the amplitude of $I_{K(erg)}$ was noted to remain unaltered. However, as cells were exposed to 10 μ M GV-58, the peak and sustained components of $I_{K(erg)}$ measured at the entire voltage-clamp ranges examined were diminished (Figure 10). For example, as the hyperpolarizing command voltage from -10 to -90 mV with a duration of 1 s was applied to the tested cell, the peak and sustained components of deactivating $I_{K(erg)}$ were significantly reduced to 283 ± 26 and 16 ± 13 pA ($n = 8$, $p < 0.05$) from control values of 336 ± 31 and 28 ± 14 pA ($n = 8$), respectively. After washout of the compound, peak and sustained $I_{K(erg)}$ was returned to 328 ± 29 and 27 ± 13 pA ($n = 7$). The mean $I-V$ relationships of peak and sustained $I_{K(erg)}$ acquired in the absence or presence of 10 μ M GV-58 were constructed and are hence presented in Figure 10B,C, respectively. However, as cells were exposed to E-4031 (10 μ M), an inhibitor of $I_{K(erg)}$, the $I_{K(erg)}$ evoked from -10 to -100 mV was fully abolished. Therefore, as compared with its effect on $I_{K(A)}$, the $I_{K(erg)}$ residing in GH₃ cells is mildly suppressed by GV-58 presence.

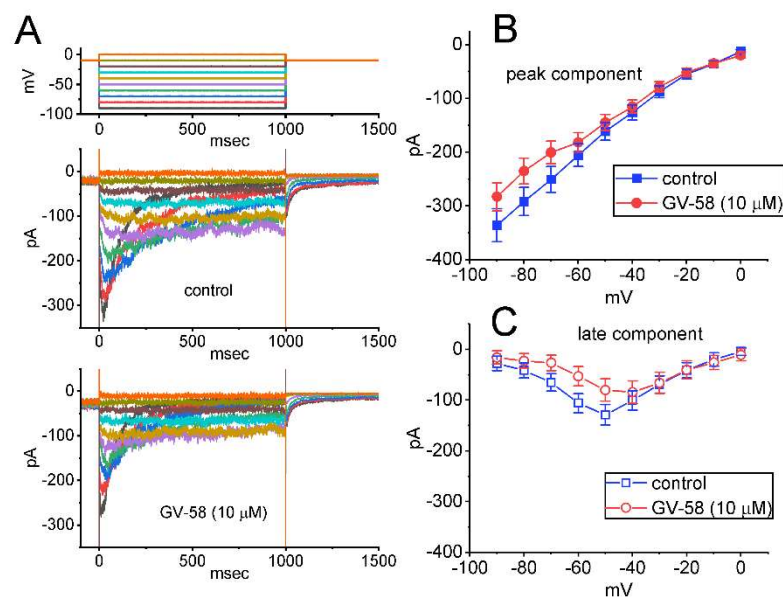


Figure 10. Effects of GV-58 on *erg*-mediated K^+ current ($I_{K(erg)}$) in GH_3 cells. In these experiments, we kept cells bathed in high- K^+ , Ca^{2+} -free solution containing $1 \mu M$ TTX, and the patch pipette was filled up with K^+ -containing solution. The composition of these solutions is elaborated in Table 1. (A) Representative current traces activated by a series of voltage pulses (indicated in the uppermost part). Current traces shown in the upper part were obtained during the control period, whereas those in the lower part were acquired in the presence of $10 \mu M$ GV-58. In (B,C), the mean current–voltage (I - V) relationships of peak (upper, filled symbols) and sustained (lower, open symbols) components of $I_{K(erg)}$ achieved in the absence (square symbols) or presence (circle symbols) of $10 \mu M$ GV-58 are illustrated, respectively. The peak and sustained components of $I_{K(erg)}$ were measured at the beginning and end-pulse of each voltage pulse, respectively. Each bar in (B,C) represents the mean \pm SEM ($n = 8$). Of notice, the presence of $10 \mu M$ GV-58 mildly suppresses the magnitude of $I_{K(erg)}$ in these cells.

3.11. Stimulatory Effect of GV-58 on Spontaneous Action Potentials (Aps) Recorded from GH_3 Cells

In another set of experiments, we performed current-clamp potential recordings in order to examine any changes in membrane potential of these cells during the absence or presence of GV-58. We kept cells bathed in normal Tyrode's solution containing 1.8 mM $CaCl_2$, and the recording electrode was filled up with K^+ -containing solution. One minute after cells were exposed to GV-58 at a concentration of 1 or $3 \mu M$, the AP firing recorded under current-clamp configuration was progressively raised (Figure 11). For example, GV-58 ($3 \mu M$) resulted in a striking increase in the firing frequency of APs from 0.85 ± 0.05 to $1.52 \pm 0.07 \text{ Hz}$ ($n = 7$, $p < 0.05$). As the compound was removed, the frequency was returned to $0.88 \pm 0.06 \text{ Hz}$ ($n = 6$). However, ω -conotoxin MVIID (100 nM) alone had no effect on AP firing. Moreover, the further addition of ranolazine ($10 \mu M$), but in continued presence of $3 \mu M$ GV-58, was effective in suppressing the frequency of spontaneous APs observed in GH_3 cells. It is, thus, possible from the current experiments that GV-58-stimulated increase in AP firing is predominantly linked to its excitatory actions on I_{Na} , $I_{Na(R)}$, and $I_{Na(W)}$ yet not solely by the agonistic effect on Ca_V channels stated previously [2–5].

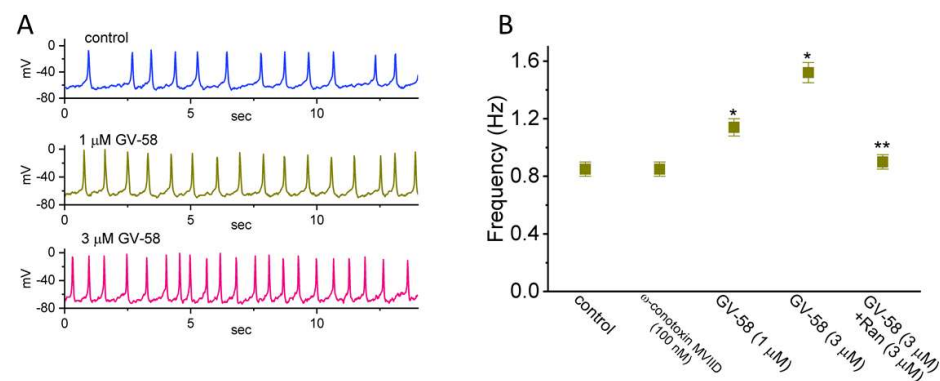


Figure 11. Effects of GV-58 on spontaneous action potentials (APs) recorded from GH₃ cells. Cells were bathed in normal Tyrode's solution, and the recording pipettes were filled with K⁺-containing solution. When whole-cell configuration was established, we switched to the whole-cell current clamp recordings to measure changes in membrane potential, as current was set at zero. (A) Representative potential traces achieved in the absence (upper) and presence of 1 μM GV-58 (middle) or 3 μM GV-58 (lower). (B) Summary graph demonstrating effect of ω-conotoxin MVIID, GV-58, and GV-58 plus ranolazine (Ran) on the firing frequency of APs in GH₃ cells (mean ± SEM; n = 8). * Significantly different from control ($p < 0.05$) and ** Significantly different from GV-58 (3 μM) alone group ($p < 0.05$). Statistical analyses were made in one-way ANOVA among different groups ($p < 0.05$).

3.12. Effect of GV-58 on I_{Na} Inherently in NSC-34 Motor Neuron-like Cells

GV-58 was previously reported to enhance spontaneous and evoked activity in the ventral horn of the spinal cord [4]. For these reasons, a final stage of experiments was undertaken to determine whether the I_{Na} present in NSC-34 motor neuron-like cells [32] can be vulnerable to any modification by the existence of GV-58. Consistent with the observations made above in GH₃ cells, the I_{Na} in NSC-34 cells can be enhanced during exposure to GV-58 (Figure 12A,B). For example, as NSC-34 cells were exposed to 3 μM GV-58, the peak amplitude of I_{Na} activated by abrupt depolarizing pulse from −100 to −10 mV was conceivably raised to 587 ± 38 pA ($n = 7$, $p < 0.05$) from a control value of 456 ± 27 pA ($n = 7$). Moreover, as GV-58 was continually present, subsequent addition of riluzole (10 μM) strikingly reduced the magnitude of GV-58-stimulated I_{Na} in NSC-34 cells (Figure 12B). Riluzole has been reportedly demonstrated to suppress I_{Na} effectively and to be useful in the management of amyotrophic lateral sclerosis or degenerative cervical myelopathy [33–35]. These experimental observations reflect that the ameliorating effect of GV-58 on neuromuscular weakness could partly derive from its stimulation of I_{Na} demonstrated herein, although the overarching activation of neuronal Ca_v channels caused by this compound has been demonstrated [2–5].

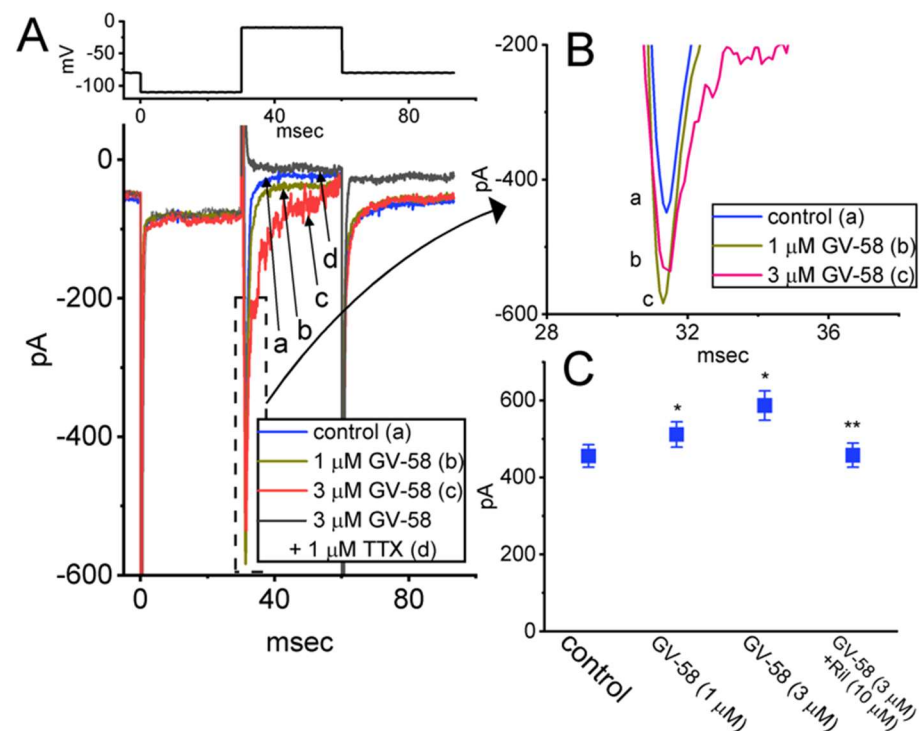


Figure 12. Effects of GV-58 on I_{Na} identified in NSC-34 motor neuron-like cells. These experiments were undertaken in cells bathed in Ca^{2+} -free Tyrode's solution which contained 10 mM TEA and 0.5 mM $CdCl_2$, while the recording pipettes that we prepared were filled up with Cs^+ -containing solution. (A) Representative I_{Na} traces obtained in the control (a), during cell exposure to 1 μ M GV-58 (b) or 3 μ M GV-58 (c), and in the presence of 3 μ M GV-58 plus 1 μ M TTX (d). The upper part in (A) depicts the voltage-clamp protocol applied. In (B), an expanded record showing I_{Na} traces is taken from the dashed box in (A). (C) Summary graph showing effect of GV-58 (1 or 3 μ M) and GV-58 (3 μ M) plus riluzole (Ril, 10 μ M). Current amplitude was taken at the beginning of depolarizing command voltage from -100 to -10 mV with a duration of 30 ms. Each bar indicates the mean \pm SEM ($n = 7$). * Significantly different from control ($p < 0.05$) and ** Significantly different from GV-58 (3 μ M) alone group ($p < 0.05$). Statistical analyses were made in one-way ANOVA among different groups ($p < 0.05$).

4. Discussion

The notable findings in this work are that: (a) GH₃ cell exposure to GV-58 could differentially increase peak and late components of I_{Na} activated by abrupt step depolarization in a concentration-, time-, and state-dependent manner (Figure 1); (b) the I_{Na} activated by brief depolarizing pulse was sensitive to either blockage by tetrodotoxin or stimulation by GV-58, but it failed to be affected by ω -conotoxin MVIID (Figure 3) (however, no change in the steady-state $I-V$ relation of peak I_{Na} in the presence of GV-58 was noted (Figure 2)); (c) the recovery of I_{Na} inactivation induced with varying interpulse intervals was enhanced in its presence, while I_{Na} decay evoked by a train of depolarizing pulses became slowed (Figure 4); (d) the decline of peak I_{Na} during rapid repetitive stimuli was slowed in the presence of GV-58 (Figure 5), while this compound stimulated peak I_{Na} in a tonic and use-dependent manner (Figure 6); (e) cell exposure to GV-58 was able to enhance $I_{Na(R)}$ and $I_{Na(W)}$ evoked by the descending and ascending ramp pulses, respectively (Figures 7 and 8); (f) the presence of this compound decreased $I_{K(A)}$ together with an increase in inactivation rate of the current, while it mildly reduced $I_{K(erg)}$ measured throughout the entire voltage-clamp steps delivered (Figures 9 and 10); (g) GV-58 increased the frequency of spontaneous APs recorded under current-clamp conditions (Figure 11); and (h) the I_{Na} amplitude in NSC-34 motor neuron-like cells could be enhanced by adding GV-58 (Figure 12). The mRNA transcripts for the α -subunit of $Nav1.1$, $Nav1.2$, and $Nav1.6$ were reported to be

present in GH₃ cells [11]. Together, findings from this study can be interpreted to reflect that the presence of GV-58 can stimulate the amplitude and gating of I_{Na} and that it would engage in the modifications of spontaneous APs in electrically excitable cells (e.g., GH₃ or NSC-34 cells), presuming that similar *in vivo* results occur.

In the current study, we disclosed that the presence of GV-58 was able to increase recovery of I_{Na} inactivation evoked in response to varying interpulse intervals in a geometrics-based progression; however, it slowed down current inactivation activated during pulse-train stimulation. Therefore, the post-spike I_{Na} during rapid repetitive stimuli is virtually linked to the prominent slow inactivation in GH₃ cells, suggesting such slow inactivation develops from open channels, and, if recovery from slow inactivation occurs through the open state (conformation), it would be accompanied by a small residual steady current. The presence of GV-58 would be anticipated to enhance the magnitude of post-spike and steady currents, hence raising the occurrence of subthreshold potential [21,24,36,37]. Likewise, the magnitude of ramp-induced $I_{Na(R)}$ and $I_{Na(W)}$ residing in GH₃ cells was expected to become elevated during exposure to GV-58. The simulation by GV-58 of firing frequency recorded under current-clamp experiments is consistent with a previous study made on microelectrode arrays [4]. It is thus reasonable to assume that the GV-58 molecule may have a higher affinity to the open/inactivated state than to the resting (closed) state residing in the Na_V channels, although the detailed ionic mechanism of its stimulatory actions on this channel warrants further detailed investigations.

GV-58 has been previously shown to be more potent on N- and P/Q-type Ca²⁺ channels with an EC₅₀ of 6.8 and 9.9 μM, respectively, over L-type Ca²⁺ channels (EC₅₀ > 100 μM) [1]. Additionally, several lines of evidence have been revealed to indicate that GV-58 can stimulate N- and P/Q-type Ca²⁺ currents [2–5]. Pituitary cells have been demonstrated to functionally express two components of Ca_V-channel currents found in GH₃ cells [11,38,39]. As such, the question arises as to whether the stimulatory effect of GV-58 on I_{Na} or AP firing observed in GH₃ cells may actually result from the activation of Ca²⁺ currents. However, this notion appears to be difficult to reconcile with the current observations revealing that ω-conotoxin MVIID, a blocker of N- and P/Q-type Ca_V-channel currents [20], failed to suppress I_{Na} and that further addition of ranolazine, an inhibitor of late I_{Na} [16,19], was able to counteract GV-58-stimulated AP firing. It is also important to notice that GV-58 could not only inhibit the amplitude of $I_{K(A)}$ but also decrease the inactivation time constant of the current, although it mildly suppressed $I_{K(erg)}$. Therefore, under our experimental conditions, the stimulation of I_{Na} , $I_{Na(R)}$, and $I_{Na(W)}$ produced by GV-58 tends to occur in a manner largely unlinked to its agonistic actions on Ca_V-channel currents. The GV-58 molecule can exert an interaction at the binding site(s) residing preferentially on Na_V channels. In this scenario, the accentuation of spontaneous APs caused by the GV-58 existence could result primarily from the accentuation of I_{Na} , including peak or late I_{Na} , $I_{Na(R)}$, and $I_{Na(W)}$.

Concentration-dependent stimulation of peak and late I_{Na} with effective EC₅₀ values of 8.9 and 2.6 μM was, respectively, observed in the presence of GV-58. As cells were exposed to GV-58, the amplitude of peak I_{Na} was increased in combination with a substantial increase in the $\tau_{inact(S)}$ value of I_{Na} activation in response to abrupt membrane depolarization. It is also worth noting, from the present observations, that, since EC₅₀ values detected in this study tend to be lower than EC₅₀ needed for its activation of N- and P/Q-type Ca_V channels [1], the GV-58 actions on I_{Na} and $I_{K(A)}$ reported herein are thus likely to be therapeutically or pharmacologically relevant. Moreover, in our study, in NSC-34 motor neuron-like cells, the exposure to GV-58 not only augmented peak and late I_{Na} but also raised the inactivation time constant of the current. However, whether GV-58-induced amelioration of neuromuscular weakness is pertinent to its stimulatory effect on the amplitude and/or kinetic gating of I_{Na} intrinsically in motor neurons needs to be further delineated. Alternatively, to what extent other structurally related compounds of GV-58 (e.g., ML-50 or GV-05) have any propensity to influence the amplitude and gating of I_{Na} is also worthy of being explored further.

In view of the experimental observations demonstrated herein, the perturbations by GV-58 of transmembrane ionic currents such as I_{Na} and $I_{K(A)}$ tend to be important and, thus, lend credence to the notion that those actions might be in part associated with its actions on the behaviors (e.g., spontaneous APs) in electrically excitable cells [15,36]. The loss of function in I_{Na} (e.g., $Na_V1.4$ -encoded current) has been recently demonstrated to be intimately linked to different neuromuscular disorders (e.g., sodium channel weakness or sodium channel myotonia) [40]. Treatment with 3,4-diaminopyridine base was also revealed to be effective in improving muscle weakness of Lambert–Eaton myasthenia [27]. Awareness thus needs to be stressed in attributing its growing use specifically to the selective agonistic effect on N- and P/Q-type Ca_V channels, since previous studies appear to underscore the importance of the increase in I_{Na} and the decrease in $I_{K(A)}$ during the presence of GV-58.

Author Contributions: Conceptualization, S.-N.W., P.-C.C., H.-Y.C., T.-H.C. and M.-C.Y.; methodology, S.-N.W.; software, S.-N.W.; validation, P.-C.C., H.-Y.C., T.-H.C. and S.-N.W.; formal analysis, S.-N.W.; investigation, H.-Y.C., T.-H.C., M.-C.Y. and S.-N.W.; resources, S.-N.W.; data curation, S.-N.W.; writing—original draft preparation, S.-N.W.; writing—review and editing, P.-C.C., H.-Y.C., T.-H.C. and S.-N.W.; visualization, P.-C.C., H.-Y.C., T.-H.C. and S.-N.W.; supervision, S.-N.W. and P.-C.C.; project administration, S.-N.W. and P.-C.C.; funding acquisition, S.-N.W. All authors have read and agreed to the published version of the manuscript.

Funding: Financial support from the project MOST-110-2320-B-006-028 (Ministry of Science and Technology, Taiwan) is gratefully acknowledged.

Institutional Review Board Statement: Not applicable.

Informed Consent Statement: Not applicable.

Data Availability Statement: The original data are available upon reasonable request to the corresponding author.

Acknowledgments: H.-Y.C. and T.-H.C. received the student assistantship from the Ministry of Science and Technology, Taiwan. The authors would like to thank Zi-Han Gao for her technical assistance in this study.

Conflicts of Interest: The authors declare no competing interests that are directly relevant to this study.

Abbreviations

ANOVA	analysis of variance
AP	action potential
Ca_V channel	voltage-gated Ca^{2+} channel
EC_{50}	concentration required for 50% stimulation
<i>erg</i>	<i>ether-à-go-go</i> -related gene
GV-58	(2R)-2-[(6-[(5-methylthiophen-2-yl)methyl]amino)-9-propyl-9H-purin-2-yl]amino]butan-1-ol
$I-V$	current versus voltage
$I_{Ca,L}$	L-type Ca^{2+} current
$I_{K(A)}$	A-type K^+ current
$I_{K(erg)}$	<i>erg</i> -mediated K^+ current
I_{Na}	voltage-gated Na^+ current
$I_{Na(R)}$	resurgent I_{Na}
$I_{Na(W)}$	window I_{Na}
Na_V channel	voltage-gated Na^+ channel
Ran	ranolazine
Ril	riluzole
$\tau_{inact(S)}$	slow component in the inactivation rate constant
TTX	tetrodotoxin

References

1. Tarr, T.B.; Valdomir, G.; Liang, M.; Wipf, P.; Meriney, S.D. New calcium channel agonists as potential therapeutics in Lambert-Eaton myasthenic syndrome and other neuromuscular diseases. *Ann. N. Y. Acad. Sci.* **2012**, *1275*, 85–91. [[CrossRef](#)] [[PubMed](#)]
2. Tarr, T.B.; Malick, W.; Liang, M.; Valdomir, G.; Frasso, M.; Lacomis, D.; Reddel, S.W.; Garcia-Ocano, A.; Wipf, P.; Meriney, S.D. Evaluation of a novel calcium channel agonist for therapeutic potential in Lambert-Eaton myasthenic syndrome. *J. Neurosci.* **2013**, *33*, 10559–10567. [[CrossRef](#)] [[PubMed](#)]
3. Tarr, T.B.; Lacomis, D.; Reddel, S.W.; Liang, M.; Valdomir, G.; Frasso, M.; Wipf, P.; Meriney, S.D. Complete reversal of Lambert-Eaton myasthenic syndrome synaptic impairment by the combined use of a K⁺ channel blocker and a Ca²⁺ channel agonist. *J. Physiol.* **2014**, *592*, 3687–3696. [[CrossRef](#)] [[PubMed](#)]
4. Black, B.J.; Atmaramani, R.; Pancrazio, J.J. Spontaneous and Evoked Activity from Murine Ventral Horn Cultures on Microelectrode Arrays. *Front. Cell Neurosci.* **2017**, *11*, 304. [[CrossRef](#)] [[PubMed](#)]
5. Tyagi, S.; Bendrick, T.R.; Filipova, D.; Papadopoulos, S.; Bannister, R.A. A mutation in Ca(V)2.1 linked to a severe neurodevelopmental disorder impairs channel gating. *J. Gen. Physiol.* **2019**, *151*, 850–859. [[CrossRef](#)] [[PubMed](#)]
6. Liang, M.; Tarr, T.B.; Bravo-Altamirano, K.; Valdomir, G.; Rensch, G.; Swanson, L.; DeStefino, N.R.; Mazzarisi, C.M.; Olszewski, R.A.; Wilson, G.M.; et al. Synthesis and biological evaluation of a selective N- and p/q-type calcium channel agonist. *ACS Med. Chem. Lett.* **2012**, *3*, 985–990. [[CrossRef](#)]
7. Tarr, T.B.; Wipf, P.; Meriney, S.D. Synaptic Pathophysiology and Treatment of Lambert-Eaton Myasthenic Syndrome. *Mol. Neurobiol.* **2015**, *52*, 456–463. [[CrossRef](#)]
8. Meriney, S.D.; Tarr, T.B.; Ojala, K.S.; Wu, M.; Li, Y.; Lacomis, D.; Garcia-Ocaña, A.; Liang, M.; Valdomir, G.; Wipf, P.; et al. Lambert-Eaton myasthenic syndrome: Mouse passive-transfer model illuminates disease pathology and facilitates testing therapeutic leads. *Ann. N. Y. Acad. Sci.* **2018**, *1412*, 73–81. [[CrossRef](#)]
9. Wu, M.; White, H.V.; Boehm, B.; Meriney, C.J.; Kerrigan, K.; Frasso, M.; Liang, M.; Gotway, E.M.; Wilcox, M.R.; Johnson, J.W.; et al. New Cav2 calcium channel gating modifiers with agonist activity and therapeutic potential to treat neuromuscular disease. *Neuropharmacology* **2018**, *131*, 176–189. [[CrossRef](#)]
10. Catterall, W.A.; Goldin, A.L.; Waxman, S.G. International Union of Pharmacology.XLVII.Nomenclature and structure-function relationships of voltage-gated sodium channels. *Pharmacol. Rev.* **2005**, *57*, 397–409. [[CrossRef](#)]
11. Stojilkovic, S.S.; Tabak, J.; Bertram, R. Ion channels and signaling in the pituitary gland. *Endocr. Rev.* **2010**, *31*, 845–915. [[CrossRef](#)] [[PubMed](#)]
12. Wu, S.-N.; Chen, B.-S.; Hsu, T.-I.; Peng, H.; Wu, Y.-H.; Lo, Y.-C. Analytical studies of rapidly inactivating and noninactivating sodium currents in differentiated NG108-15 neuronal cells. *J. Theor. Biol.* **2009**, *259*, 828–836. [[CrossRef](#)] [[PubMed](#)]
13. Wu, S.N.; Wu, Y.H.; Chen, B.S.; Lo, Y.C.; Liu, Y.C. Underlying mechanism of actions of tefluthrin, a pyrethroid insecticide, on voltage-gated ion currents and on action currents in pituitary tumor (GH3) cells and GnRH-secreting (GT1-7) neurons. *Toxicology* **2009**, *258*, 70–77. [[CrossRef](#)] [[PubMed](#)]
14. Lai, M.C.; Wu, S.N.; Huang, C.W. Telmisartan, an Antagonist of Angiotensin II Receptors, Accentuates Voltage-Gated Na(+) Currents and Hippocampal Neuronal Excitability. *Front. Neurosci.* **2020**, *14*, 902. [[CrossRef](#)]
15. Chuang, T.H.; Cho, H.Y.; Wu, S.N. Effective Accentuation of Voltage-Gated Sodium Current Caused by Apocynin (4'-Hydroxy-3'-methoxyacetophenone), a Known NADPH-Oxidase Inhibitor. *Biomedicines* **2021**, *9*, 1146. [[CrossRef](#)]
16. Chen, B.S.; Lo, Y.C.; Peng, H.; Hsu, T.I.; Wu, S.N. Effects of ranolazine, a novel anti-anginal drug, on ion currents and membrane potential in pituitary tumor GH(3) cells and NG108-15 neuronal cells. *J. Pharmacol. Sci.* **2009**, *110*, 295–305. [[CrossRef](#)]
17. Chang, W.T.; Wu, S.N. Characterization of Direct Perturbations on Voltage-Gated Sodium Current by Esaxerenone, a Nonsteroidal Mineralocorticoid Receptor Blocker. *Biomedicines* **2021**, *9*, 549. [[CrossRef](#)]
18. Chen, P.C.; Ruan, J.S.; Wu, S.N. Evidence of Decreased Activity in Intermediate-Conductance Calcium-Activated Potassium Channels During Retinoic Acid-Induced Differentiation in Motor Neuron-Like NSC-34 Cells. *Cell. Physiol. Biochem.* **2018**, *48*, 2374–2388. [[CrossRef](#)]
19. So, E.C.; Wu, S.-N.; Lo, Y.-C.; Su, K. Differential regulation of tefluthrin and telmisartan on the gating charges of I(Na) activation and inactivation as well as on resurgent and persistent I(Na) in a pituitary cell line (GH(3)). *Toxicol. Lett.* **2018**, *285*, 104–112. [[CrossRef](#)]
20. Gandía, L.; Lara, B.; Imperial, J.S.; Villarroya, M.; Albillos, A.; Maroto, R.; Garcia, A.G.; Olivera, B.M. Analogies and differences between omega-conotoxins MVIIC and MVIID: Binding sites and functions in bovine chromaffin cells. *Pflugers Arch.* **1997**, *435*, 55–64.
21. Taddese, A.; Bean, B.P. Subthreshold sodium current from rapidly inactivating sodium channels drives spontaneous firing of tuberomammillary neurons. *Neuron* **2002**, *33*, 587–600. [[CrossRef](#)]
22. Kuo, P.-C.; Kao, Z.-H.; Lee, S.-W.; Wu, S.-N. Effects of Sesamin, the Major Furofuran Lignan of Sesame Oil, on the Amplitude and Gating of Voltage-Gated Na(+) and K(+) Currents. *Molecules* **2020**, *25*, 3062. [[CrossRef](#)] [[PubMed](#)]
23. Lewis, A.H.; Raman, I.M. Resurgent current of voltage-gated Na(+) channels. *J. Physiol.* **2014**, *592*, 4825–4838. [[CrossRef](#)] [[PubMed](#)]
24. Wu, S.N. Contribution of non-inactivating Na⁺ current induced by oxidizing agents to the firing behavior of neuronal action potentials: Experimental and theoretical studies from NG108-15 neuronal cells. *Chin. J. Physiol.* **2011**, *54*, 19–29. [[CrossRef](#)]

25. Morris, C.E.; Boucher, P.A.; Joós, B. Left-shifted nav channels in injured bilayer: Primary targets for neuroprotective nav antagonists? *Front. Pharmacol.* **2012**, *3*, 19. [[CrossRef](#)] [[PubMed](#)]
26. Chuang, T.-H.; Cho, H.-Y.; Wu, S.-N. The Evidence for Sparsentan-Mediated Inhibition of INa and IK(erg): Possibly Unlinked to Its Antagonism of Angiotensin II or Endothelin Type a Receptor. *Biomedicines* **2022**, *10*, 86. [[CrossRef](#)] [[PubMed](#)]
27. Sanders, D.B.; Juel, V.C.; Harati, Y.; Smith, A.G.; Peltier, A.C.; Marburger, T.; Lou, J.; Pascuzzi, R.M.; Richman, D.P.; Xie, T.; et al. 3,4-diaminopyridine base effectively treats the weakness of Lambert-Eaton myasthenia. *Muscle Nerve* **2018**, *57*, 561–568. [[CrossRef](#)]
28. Simasko, S.M. Evidence for a delayed rectifier-like potassium current in the clonal rat pituitary cell line GH3. *Am. J. Physiol.* **1991**, *261 Pt 1*, E66–E75. [[CrossRef](#)]
29. Huang, C.W.; Huang, C.C.; Liu, Y.C.; Wu, S.N. Inhibitory effect of lamotrigine on A-type potassium current in hippocampal neuron-derived H19-7 cells. *Epilepsia* **2004**, *45*, 729–736. [[CrossRef](#)]
30. Liu, P.Y.; Chang, W.T.; Wu, S.N. Characterization of the Synergistic Inhibition of I(K(erg)) and I(K(DR)) by Ribociclib, a Cyclin-Dependent Kinase 4/6 Inhibitor. *Int. J. Mol. Sci.* **2020**, *21*, 8078. [[CrossRef](#)]
31. Cho, H.Y.; Chuang, T.H.; Wu, S.N. Effective Perturbations on the Amplitude and Hysteresis of Erg-Mediated Potassium Current Caused by 1-Octylnonyl 8-[(2-hydroxyethyl)[6-oxo-6(undecyloxy)hexyl]amino]-octanoate (SM-102), a Cationic Lipid. *Biomedicines* **2021**, *9*, 1367. [[CrossRef](#)] [[PubMed](#)]
32. Wu, S.N.; Yeh, C.C.; Huang, H.C.; So, E.C.; Lo, Y.C. Electrophysiological characterization of sodium-activated potassium channels in NG108-15 and NSC-34 motor neuron-like cells. *Acta Physiol.* **2012**, *206*, 120–134. [[CrossRef](#)] [[PubMed](#)]
33. Wang, Y.-J.; Lin, M.-W.; Lin, A.-A.; Wu, S.-N. Riluzole-induced block of voltage-gated Na⁺ current and activation of BKCa channels in cultured differentiated human skeletal muscle cells. *Life Sci.* **2008**, *82*, 11–20. [[CrossRef](#)] [[PubMed](#)]
34. Chiò, A.; Mazzini, L.; Mora, G. Disease-modifying therapies in amyotrophic lateral sclerosis. *Neuropharmacology* **2020**, *167*, 107986. [[CrossRef](#)]
35. Fehlings, M.G.; Badhiwala, J.H.; Ahn, H.; Farhadi, H.F.; I Shaffrey, C.; Nassr, A.; Mummaneni, P.; Arnold, P.M.; Jacobs, W.B.; Riew, K.D.; et al. Safety and efficacy of riluzole in patients undergoing decompressive surgery for degenerative cervical myelopathy (CSM-Protect): A multicentre, double-blind, placebo-controlled, randomised, phase 3 trial. *Lancet Neurol.* **2021**, *20*, 98–106. [[CrossRef](#)]
36. Simasko, S.M. A background sodium conductance is necessary for spontaneous depolarizations in rat pituitary cell line GH3. *Am. J. Physiol.* **1994**, *266 Pt 1*, C709–C719. [[CrossRef](#)]
37. Wu, N.; Hsiao, C.F.; Chandler, S.H. Membrane resonance and subthreshold membrane oscillations in mesencephalic V neurons: Participants in burst generation. *J. Neurosci.* **2001**, *21*, 3729–3739. [[CrossRef](#)]
38. Herrington, J.; Stern, R.C.; Evers, A.; Lingle, C. Halothane inhibits two components of calcium current in clonal (GH3) pituitary cells. *J. Neurosci.* **1991**, *11*, 2226–2240. [[CrossRef](#)]
39. Lo, Y.-K.; Wu, S.-N.; Lee, C.-T.; Li, H.-F.; Chiang, H.-T. Characterization of action potential waveform-evoked L-type calcium currents in pituitary GH3 cells. *Pflugers Arch.* **2001**, *442*, 547–557. [[CrossRef](#)]
40. Nicole, S.; Lory, P. New Challenges Resulting From the Loss of Function of Na(v)1.4 in Neuromuscular Diseases. *Front. Pharmacol.* **2021**, *12*, 751095. [[CrossRef](#)]